Journal of Hazardous Materials 172 (2009) 390–394

Contents lists available at ScienceDirect

Journal of Hazardous Materials

journal homepage: www.elsevier.com/locate/jhazmat

Ozonation of trifluralin particles: An experimental investigation with a vacuum ultraviolet photoionization aerosol time-of-flight mass spectrometer

Junwang Meng, Bo Yang, Yang Zhang, Xi Shu, Jinian Shu*

Research Center for Eco-Environmental Sciences, Chinese Academy of Sciences, Beijing, 100085, China

ARTICLE INFO

Article history:
Received 4 May 2009
Received in revised form 7 July 2009
Accepted 7 July 2009
Available online 14 July 2009

Keywords:
Pesticide
Ozonation
Trifluralin
AMS

ABSTRACT

The ozonation of trifluralin coated on azelaic acid particles is investigated with a vacuum ultraviolet photoionization aerosol time-of-flight mass spectrometer. The suspended trifluralin particles with the mean diameter of 270 nm react with ~100 ppm ozone in an aerosol reaction chamber under ambient pressure and room temperature (1 atm, 298 K). The time-of-flight mass spectra of the trifluralin particles and the solid state ozonides are obtained. The assignments of the mass spectra reveal that the major primary ozonides of trifluralin particles are 2,6-dinitro-*N*-propyl-*N*-propanoyl-4-(trifluoromethyl) benzamine and 2,6-dinitro-*N*-(propan-2(and 3)-ol)-*N*-propyl-4-(trifluoromethyl) benzamine. The major secondary ozonides of trifluralin 2-ethyl-7-nitro-5-(trifluoromethyl) benzimidazole-3-oxide, 2,6-dinitro-*N*-propyl-4-(trifluoromethyl) benzenamine and 2,6-dinitro-*N*-(formyl)-*N*-propyl-4-(trifluoromethyl) benzamine are observed. The primary ozonides are directly resulted from the oxidation of *N*-propyl groups. The pathways of the primary ozonation are proposed in the paper.

1. Introduction

Pesticides are emitted into the atmosphere directly during application and indirectly through volatilization from ground, leaf surface and water. In the atmosphere, these organics not only exist in gaseous phase, some of them, especially for those with low vapor pressure, also may attach to the surface of aerosols or form secondary aerosols [1–5]. These compounds are mainly removed from the atmosphere by dry and wet deposition and chemical reactions including photolysis and reaction with oxidants [1,6,7].

Trifluralin, a selective pre-sowing and pre-emergence herbicide, is one of the most common herbicides used to control many annual grasses and broadleaf weeds for agricultural crops [8]. Once applied in the field, trifluralin immediately volatilizes into air with a large flux before soil incorporation [9]. Seasonal trifluralin releases into the atmosphere can be as high as 25% of that applied and the maximum residues of trifluralin in the air above treated fields are in the range of 2–3 $\mu g\,m^{-3}$ following application [10]. Trifluralin, a persistent compound in the atmosphere [11], was found in air, rainwater and microlayer [12,13]. The particle phase of trifluralin accounted for ~3% of total trifluralin in the atmosphere [14].

The early studies mainly focused on the environmental fate of trifluralin under various physical and biological conditions [15–19]. These research results showed that the two *N*-propyl groups of trifluralin are relatively reactive and the oxidation of the propyl groups resulted in the formation of the hydroxyl and carbonyl groups [18,19]. Recently, the degradation of trifluralin by Fe(II) in solution and the reaction of trifluralin with ozone in the trifluralin-contaminated soil and the OH radical in the gas phase have been reported [8,20,21]. Pierpoint et al. reported the observation of the oxidation and cleavage of the *N*-propyl groups and several ozonides in trifluralin-contaminated soil treated with ozone [20]. The photolysis of trifluralin in the gas phase and coated on the fly ash and kaolin was reported [21,22]. Ozone is one of the major oxidants in the atmosphere which can degrade many compounds. The ozonation of trifluralin absorbed on the surface of the ambient aerosol particles may affect the total environmental fate of trifluralin. However, to the best of our knowledge, no investigation on the ozonation of particle-phase trifluralin has been reported yet.

In the present study, we have conducted a real-time investigation on the ozonation of trifluralin particles with a vacuum ultraviolet photoionization aerosol time-of-flight mass spectrometer (VUV-ATOFMS). The time-of-flight mass spectra of the trifluralin particles and the solid state ozonides are acquired with the VUV-ATOFMS. Combining with the previous studies on the trifluralin, the mass spectra are tentatively assigned. The major pathways of ozonation of trifluralin are proposed in the paper.

2. Experimental

The schematic diagram of the experimental setup is shown in Fig. 1. The aerosol reaction chamber consists of a cylindrical

* Corresponding author. Tel.: +86 010 6284 9508; fax: +86 010 6292 3563.
E-mail address: jshu@rcees.ac.cn (J. Shu).

0304-3894/$ – see front matter © 2009 Elsevier B.V. All rights reserved.
doi:10.1016/j.jhazmat.2009.07.020

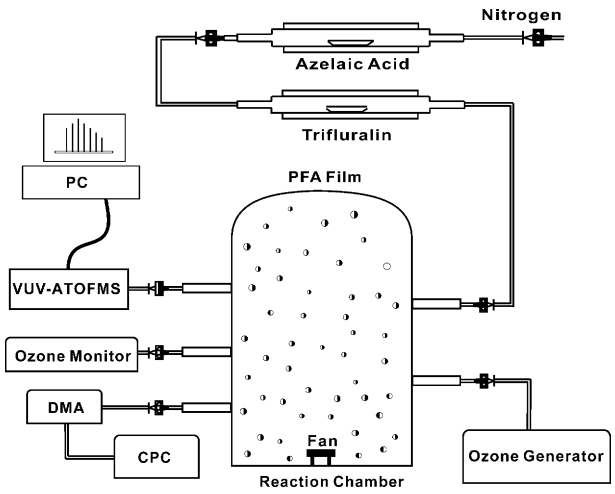

Fig. 1. Schematic diagram of the experimental set-up.

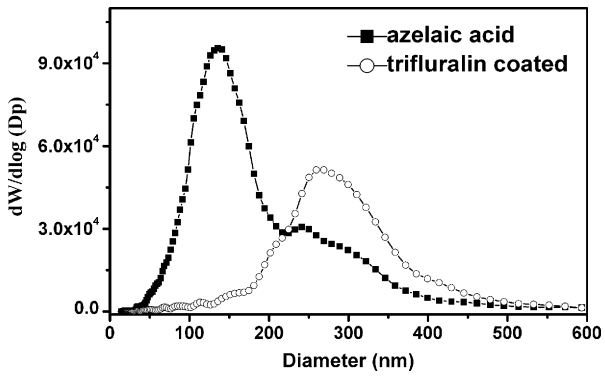

Fig. 2. Particle size distributions of azelaic acid particles and trifluralin-coated particles measured by SMPS.

stainless steel chamber (Ø50 cm × H60 cm) and a thin perfluoroalkoxy (PFA) film (Ø51 cm × H50 cm) bag on the top of the chamber. The PFA bag is used to keep one atmospheric pressure in the aerosol reaction chamber during the experiment. A small fan is set at the bottom of the aerosol reaction chamber to mix the reactants quickly. Prior to each experiment, the reaction chamber is cleaned for several hours with filter air. The relative humidity in the chamber is estimated to be ~5% due to the residual filtered ambient air in the chamber. The size distributions and concentrations of the particles are measured with a scanning mobility particle sizer (SMPS), which is composed of a differential mobility analyzer (DMA, TSI model 3081) and a condensation particle counter (CPC, TSI model 3776). Conductive silicone tubes (TSI) are used to deliver particles between each instrument in order to minimize the wall loss of the particles during transportation. Ozone is generated with an ozone generator (NIPPON, model NPF8W). Pure oxygen (99.99%) is used as the discharging gas. The flow of the discharging gas is maintained at 5 lpm with a ball-float flowmeter. The concentration of ozone in the reaction chamber is controlled by adjusting the feed-in time of the discharged gas and detected with an ozone monitor (2B technologies Inc., model 201M).

The VUV-ATOFMS used to analyze the trifluralin and the ozonides is home-built and a detailed description has been given elsewhere [23]. Information only directly related to the present work is described here. A nozzle of ~0.12 mm orifice combined with an aerodynamic lens assembly and a three stage differential pumping system is used to sample particles directly at atmospheric pressure. The sample rate of the VUV-ATOFMS is 1.3 cm^3 atm s^{-1}. An 8 mm diameter copper rod coupled to a cartridge heater driven by a DC power supply is used to vaporize organic particles. The heater temperature used in the experiment is ~400 K. The vapor generated from particles is photoionized with light radiated from a home-assembled RF-powered VUV lamp. The VUV irradiation is achieved by exciting a 210 Pa mixture of 5% krypton in helium (v/v) with a copper coil driven by a 13.56 MHz RF power supply. It outputs ~5×10^{14} VUV photons per second with ~30% photons confined in 0.01 sr. Then, the ions produced by VUV photoionization are detected with a reflectron mass spectrometer. The reflectron mass spectrometer is characterized with a field free flight distance of 1.4 m, an ion mirror and a chevron multichannel plate detector. The cost of the VUV-ATOFMS is about US$ 150K. The main payout is made on the purchase of the turbo pumps, the multiscaler, the RF power supply, the high voltage pulser, the pulse delay generator, and machining of the vacuum apparatus. The cost to build the VUV-ATOFMS is more expensive than buy a regular GC/MS. Nevertheless, its capability of the on-line analysis is a good supplement to the traditional off-line analytical instruments.

The suspended trifluralin particles are generated by the homogeneous nucleation method. The aerosol generator consists of two tandem 40 cm long quartz tubes with OD 3 cm wrapped with heating tapes and equipped with thermometers. About 0.2 g azelaic acid used to generate nucleus is put in a small boat-shaped ceramic container positioned at the center of the first quartz tube. Azelaic acid is chosen as the nucleus because it has little reactivity with ozone [24]. The temperature of the first quartz tube is at 408 K. Meanwhile, ~0.1 g trifluralin used to coat the azelaic acid nucleus is placed into the center of the second quartz tube. The temperature of the second tube is set at 375 K. The particle concentration and coating thickness are controlled by adjusting the temperature of the quartz tubes during the experiments. Pure nitrogen passes through the two tubes sequentially at a volumetric flow of ~0.5 lpm controlled by a ball-float flowmeter. The temperature of each quartz tube is optimized to produce aerosol particles with the expected size and mass concentration to meet the detection limit of the VUV-ATOFMS. Fig. 2 shows the polydisperse size distributions of the generated particles measured with the SMPS. The size distribution of the pure azelaic acid particles has a mean diameter of 136 nm and the mass concentration of azelaic acid particles is ~930 μg/m^3. The size distribution of the trifluralin-coated particles shifts to the mean diameters of 270 nm with the mass concentration of ~4900 μg/m^3. The large shift of the size distributions of the trifluralin particles indicates a multilayer coating of the trifluralin on the azelaic acid nucleus.

Trifluralin (~95%, Kongfeng Chemical Co. Ltd., China), azelaic acid (99%, China North Region Special Chemical Reagent Development Center), 1-butanol (>99%, Beijing Chemical works) and 2-butanone (>99%, Beijing Chemical Works) are used in the experiment. Oxygen (99.99%) and nitrogen (99.99%) are purchased from Beijing Huayuan Gas Chemical Industry Co. Ltd.

3. Results and discussion

The time-of-flight mass spectrum of trifluralin ($C_{13}H_{16}F_3N_3O_4$, mol. wt 335) particles is shown in Fig. 3. The mass spectrum of trifluralin particles is acquired before ozone is injected into the reaction chamber. The acquisition time for the mass spectrum is 60 s. The mass spectrum is normalized with the intensity of the mass peak at m/z 335 which is assigned to the molecular ion of trifluralin ($C_{13}H_{16}F_3N_3O_4^+$, mol. wt 335). Other prominent mass peaks shown in Fig. 3 are at m/z 318 and 306. The minor mass peaks are at m/z 290, 277, 260, 248, and 232. The intensities and tentative assignments of the mass peaks are listed in the Table 1. The prominent fragment mass peaks at m/z 306 and 318 are assigned to $C_{11}H_{11}F_3N_3O_4^+$ (C_2H_5 lose) and $C_{13}H_{15}F_3N_3O_3^+$ (OH lose), respectively. The assignments of other minor mass peaks are speculated according to the number

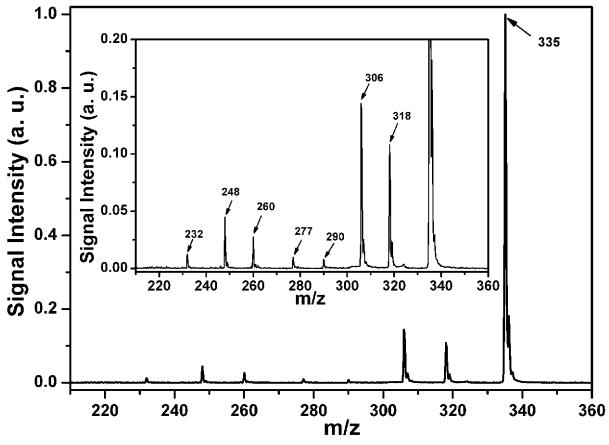

Fig. 3. Time-of-flight mass spectrum of trifluralin particles obtained with the VUV-ATOFMS. The acquisition time for the mass spectrum is 60 s. The intensities of the mass peaks are normalized with that of the mass peak at *m*/*z* 335.

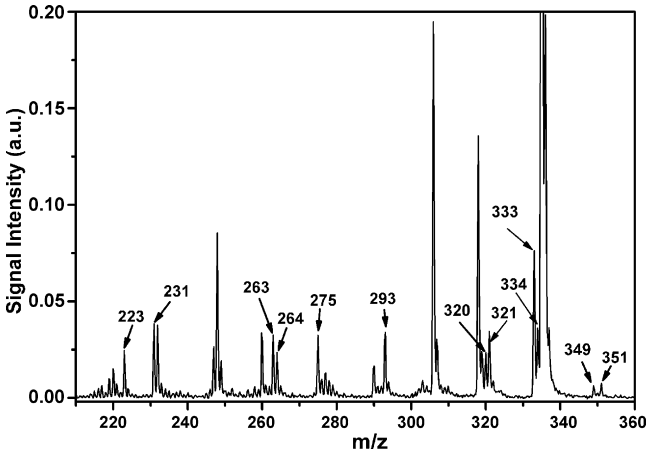

Fig. 4. Time-of-flight mass spectrum of the solid state ozonides of trifluralin particles obtained with the VUV-ATOFMS. The mass spectrum is acquired 10 min after ozone is injected into the reaction chamber. The time of acquisition is 150 s. The peak intensities are normalized with that of the peak at 335 *m*/*z*.

of *m*/*z* and the possible fragmentation of trifluralin during the VUV photoionization.

Fig. 4 shows the time-of-flight mass spectrum of the ozonation productions of trifluralin particles. The mass spectrum is collected 10 min after ozone is injected into the reaction chamber. The injection of ozone takes ~20 s. The initial concentration of ozone is ~100 ppm. The acquisition time for the mass spectrum is 150 s. Since the signal of the reaction products of trifluralin is very weak, Fig. 4 is zoomed in to a small scale to show the tiny mass peaks. Compared to the mass spectrum of trifluralin shown in the zoomed plot of Fig. 3, the new mass peaks at *m*/*z* 223, 231, 263, 264, 275, 293, 320, 321, 333, 334, 349, and 351 are observed in the mass spectrum shown in Fig. 4. The intensities and tentative assignments of the mass peaks are listed in the Table 1. The mass peak at *m*/*z* 351 is assigned to 2,6-dinitro-*N*-(propan-2(and 3)-ol)-*N*-propyl-4-(trifluoromethyl) benzamine ($C_{13}H_{16}F_3N_3O_5$, mol. wt 351). Golab et al. reported that 2,6-dinitro-*N*-(propan-2(and 3)-ol)-*N*-propyl-4-(trifluoromethyl) benzamine are two of the transformation products of trifluralin in soil, which are resulted from the hydroxylation of the propyl group at carbon-2 and carbon-3 [18]. The mass peak at *m*/*z* 349 is assigned to 2,6-dinitro-*N*-propyl-*N*-propanoyl-4-(trifluoromethyl) benzamine ($C_{13}H_{14}F_3N_3O_5$, mol. wt 349). 2,6-dinitro-*N*-propyl-*N*-propanoyl-4-(trifluoromethyl) benzamine was reported as one transformation product of trifluralin in soil, which resulted from the oxidation of the propyl group at carbon-1 [18]. Pierpoint et al. also reported that 2,6-dinitro-*N*-propyl-*N*-propanoyl-4-(trifluoromethyl) benzamine is the ozonation product of trifluralin in soil. Since 2,6-dinitro-*N*-(propan-2(and 3)-ol)-*N*-propyl-4-(trifluoromethyl) benzamine and 2,6-dinitro-*N*-propyl-*N*-propanoyl-4-(trifluoromethyl) benzamine are directly resulted from the attack of ozone on the propyl group of trifluralin, we think that they are the primary ozonation products of trifluralin. In addition, the ozonation products with mol. wt 293 and 275 have been reported in the ozonation of trifluralin in soil [20], we tentatively assigned the mass peaks at 293 and 275 to the secondary ozonides 2-ethyl-7-nitro-5-(trifluoromethyl)benzimidazole-3-oxide (mol. wt 275) and 2.6-dinitro-*N*-propyl-4-(trifluoromethyl)benzenamine (mol. wt 293).

Since the VUV photoionization mass spectrum of trifluralin shown in Fig. 3 is not fragment free, the primary ozonation products of trifluralin may also form fragment ions during the VUV photoionization. Therefore, the mass peaks from the fragment ions of primary ozonation products may overlap with those from the secondary ozonides on the mass spectra. As shown in Fig. 3, trifluralin loses readily an OH or a C_2H_5 fragment during the VUV photoionization. In order to understand the possible fragmentation of the primary ozonation products of trifluralin during the VUV photoionization, we acquire the VUV photoionization mass spectra of 1-butanol ($CH_3CH_2CH_2CH_2OH$, mol. wt 74) and 2-butanone ($CH_3CH_2CHOCH_3$, mol. wt 72) with the VUV-ATOFMS as a reference. The VUV photoionization mass spectra of 1-butanol shown in Fig. 5(a) reveals that 1-butanol is easy to dissociate and lose a H_2O during the VUV photoionization, which indicates that 2,6-dinitro-*N*-(propan-2(and 3)-ol)-*N*-propyl-4-(trifluoromethyl) benzamine may also lose a H_2O during the VUV photoionization. Therefore, 2,6-dinitro-*N*-(propan-2(and 3)-ol)-*N*-propyl-4-(trifluoromethyl) benzamine (mol. wt 351) have the possibility to lose OH, C_2H_5, or H_2O during the VUV photoionization. Thus, we tentatively assign the mass peaks at *m*/*z* 333 and 334 shown in Fig. 4 to the fragment ions of 2,6-dinitro-*N*-(propan-2(and 3)-ol)-*N*-propyl-4-(trifluoromethyl) benzamine (mol. wt 351) by losing OH and H_2O during the VUV photoionization. The VUV photoionization mass spectra of 2-butanone shown in Fig. 5(b)

Table 1
The intensities and assignments of the mass peaks of the trifluralin and its ozonides.

m/*z*	T	η	T + O	ε
351			$C_{13}H_{16}F_3N_3O_5^+$	0.01
349			$C_{13}H_{14}F_3N_3O_5^+$	0.01
335	$C_{13}H_{16}F_3N_3O_4^+$	1.00	$C_{13}H_{16}F_3N_3O_4^+$	1.00
334			$C_{13}H_{15}F_3N_3O_4^+$	0.04
333			$C_{13}H_{14}F_3N_3O_4^+$	0.08
321			$C_{11}H_{10}F_3N_3O_5^+$	0.03
320			$C_{11}H_9F_3N_3O_5^+$	0.02
318	$C_{13}H_{15}F_3N_3O_3^+$	0.11	$C_{13}H_{15}F_3N_3O_3^+$	0.14
306	$C_{11}H_{11}F_3N_3O_4^+$	0.14	$C_{11}H_{11}F_3N_3O_4^+$	0.19
293			$C_{10}H_{10}F_3N_3O_4^+$	0.03
290	$C_{11}H_{11}F_3N_3O_3^+$	0.01	$C_{11}H_{11}F_3N_3O_3^+$	0.02
277	$C_9H_6F_3N_3O_4^+$	0.01	$C_9H_6F_3N_3O_4^+$	0.01
275			$C_{10}H_8F_3N_3O_3^+$	0.03
264			$C_8H_5F_3N_3O_4^+$	0.02
263			$C_8H_4F_3N_3O_4^+$	0.03
260	$C_9H_5F_3N_3O_3^+$	0.03	$C_9H_5F_3N_3O_3^+$	0.03
248	$C_8H_5F_3N_3O_3^+$	0.04	$C_8H_5F_3N_3O_3^+$	0.09
232	$C_8H_5F_3N_3O_2^+$	0.01	$C_8H_5F_3N_3O_2^+$	0.04
231			$C_8H_4F_3N_3O_2^+$	0.04
223			$C_7H_8F_3N_3O_2^+$	0.02

The symbols of η and ε stand for the intensities of the mass peaks contributed from the trifluralin (T) and its ozonation products (T + O) shown in Figs. 3 and 4. The intensities of all the mass peaks are normalized with that of the mass peak at *m*/*z* 335.

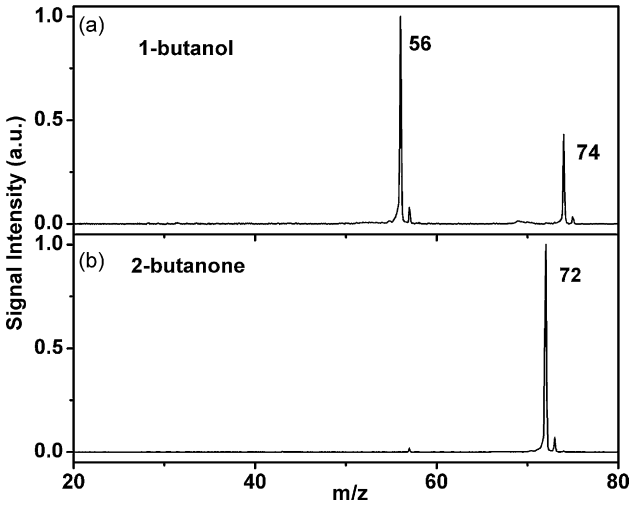

Fig. 5. Time-of-flight mass spectra of 1-butanol and 2-butone obtained with the VUV-ATOFMS. The mass spectrum of 1-butanol is normalized with the intensity of the mass peak at *m*/*z* 56 while the mass spectrum of 2-butone is normalized with the intensity of the mass peak at *m*/*z* 72.

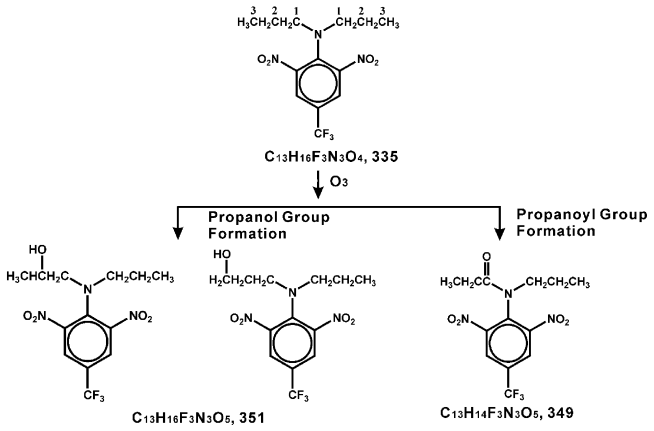

Fig. 6. The proposed pathways of the ozonation of trifluralin particles.

shows a very small fragment ion peak at *m*/*z* 57 with the relative intensity of ~0.02 compared to that of the molecular ion, which corresponds to the daughter ion of butanone by losing a CH_3 group. Therefore, we speculate that 2,6-dinitro-*N*-propyl-*N*-propanoyl-4-(trifluoromethyl) benzamine ($C_{13}H_{14}F_3N_3O_5$, mol. wt 349) may only be prone to lose OH and C_2H_5 like trifluralin during the VUV photoionization. The mass peak at *m*/*z* 320, thereby, is assigned to the daughter of 2,6-dinitro-*N*-propyl-*N*-propanoyl-4-(trifluoromethyl) benzamine by losing C_2H_5. The analyses above roughly excludes that the mass peak at *m*/*z* 321 is contributed from the daughter ion of the primary ozonides of trifluralin. We tentatively assign the mass peak at *m*/*z* 321 to 2,6-dinitro-*N*-(formyl)-*N*-propyl-4-(trifluoromethyl) benzamine ($C_{11}H_{10}F_3N_3O_5$, mol. wt 321), possibly a secondary ozonide. The mass peaks at *m*/*z* 223, 231, 263, and 264 may be contributed from either fragment ions of the ozonides or the secondary ozonides. But no proper assignments can be found for them based on the experimental data obtained in the experiment.

The oxidation of the *N*-propyl group has been observed in the ozone treatment of trifluralin-contaminated soil [20] and the natural degradation of trifluralin in soil and plants [18,19]. The formations of 2,6-dinitro-*N*-propyl-*N*-propanoyl-4-(trifluoromethyl) benzamine and 2,6-dinitro-*N*-(propan-2(and 3)-ol)-*N*-propyl-4-(trifluoromethyl) benzamine indicate that the ozonation of trifluralin is initiated by the attack of ozone on the propyl group of trifluralin. Therefore, the reaction of trifluralin with ozone may be similar to the ozonation of alkane. Even the mechanism of ozonation of the alkane is still controversial, the formation of alcohols and carbonyl compounds has been observed in the ozonation of the alkanes [25]. Based on the knowledge mentioned above, the main pathways for the ozonation of trifluralin particles are proposed in Fig. 6. The primary ozonation of trifluralin is composed of two pathways, which lead to the formation of propanoyl and propanol group on the N atom, respectively. The attacks of ozone on carbon-2 and carbon-3 of the *N*-propyl group form 2,6-dinitro-*N*-(propan-2(and 3)-ol)-*N*-propyl-4-(trifluoromethyl) benzamine, while the attack on carbon-1 forms 2,6-dinitro-*N*-propyl-N-propanoyl-4-(trifluoromethyl) benzamine. The mass peak at *m*/*z* 351 observed corresponds to the molecular ion of 2,6-dinitro-*N*-(propan-2(and 3)-ol)-*N*-propyl-4-(trifluoromethyl) benzamine. The mass peak at *m*/*z* 333 observed is the additional evidence to the formation of the propanol group, which is characterized by losing a H_2O during the VUV photoionization. The mass peak at *m*/*z* 349 corresponds to the molecular ion of 2,6-dinitro-*N*-propyl-*N*-propanoyl-4-(trifluoromethyl) benzamine. Additionally, 2,6-dinitro-*N*-propyl-*N*-propanoyl-4-(trifluoromethyl) benzamine has been found in the natural degradation of trifluralin in soil [20]. Thus, the mass peak at *m*/*z* 349 is assigned to 2,6-dinitro-*N*-propyl-*N*-propanoyl-4-(trifluoromethyl) benzamine. The propanoyl group formation of trifluralin ozonation may be similar to the ozonation of substituted cyclopropane, which exhibits a general preference for oxidation of the secondary C–H bond in the α position to the ring forming carbonyl compounds [26]. The primary ozonides of trifluralin may undergo further oxidation to form the secondary ozonides. However, this investigation cannot reveal any clear information on the molecular structures and the formation mechanism of the secondary ozonides.

Since the signal of the trifluralin ozonides is very weak, the high concentrations of ozone and trifluralin particles are applied in the experiment with the aim to produce the ozonides with the amount enough to meet the detection limit of the VUV-ATOFMS. The mass peaks of ozonides of trifluralin appear and increase slowly with time after ozone is injected into the trifluralin particles-filled reaction chamber. The intensities of the mass peaks of the ozonides reaches a maximum after 15 min later and then slowly decreases with the time perhaps due to the wall loss. The small mass peaks of ozonides and the large mass peak of trifluralin shown in Fig. 4 indicate that only the small part of trifluralin coated on azelaic acid particles takes part in the reaction during the ozonation even the ozone is in excess. We speculate that the nascent solid-phase ozonides prevent the inner layers of the trifluralin from ozonation.

4. Conclusion

In this experiment, the vacuum ultraviolet photoionization aerosol time-of-flight mass spectrometer is utilized to realize the rapid analysis of the ozonides of trifluralin. Compared to the traditional analysis methods such as GC/MS, this on-line analysis method avoids possible contamination and further reactions of the sample during preparation for the off-line analysis. However, the mass spectra obtained with the VUV-ATOFMS cannot be used to identify the chemical as GC/MS does. Referring to the previous studies on the ozonation and the natural degradation of trifluralin in soil [18,20], we tentatively assign the mass spectrum of the trifluralin ozonides. 2,6-dinitro-*N*-propyl-*N*-propanoyl-4-(trifluoromethyl) benzamine (mol. wt 349) and 2,6-dinitro-*N*-(propan-2(and 3)-ol)-*N*-propyl-4-(trifluoromethyl) benzamine (mol. wt 351) are the major primary ozonides of trifluralin particles. The major secondary ozonides of trifluralin 2-ethyl-

7-nitro-5-(trifluoromethyl) benzimidazole-3-oxide (mol. wt 275) and 2.6-dinitro-*N*-propyl-4-(trifluoromethyl)benzenamine (mol. wt 293), and 2,6-dinitro-*N*-(formyl)-*N*-propyl-4-(trifluoromethyl) benzamine (mol. wt 321) are observed. The ozonation of trifluralin is resulted from the oxidation of *N*-propyl groups. The attacks of ozone on carbon-2 and carbon-3 of the *N*-propyl group form 2,6-dinitro-*N*-(propan-2(and 3)-ol)-*N*-propyl-4-(trifluoromethyl) benzamine, while the attack on carbon-1 forms 2,6-dinitro-*N*-propyl-*N*-propanoyl-4-(trifluoromethyl) benzamine.

Acknowledgment

This work was funded by Creative Research Groups of China (grant no. 50621804) and National Natural Science Foundation of China (grant no. 20673138).

References

[1] W.A.J. van Pul, T.F. Bidleman, E. Brorstrom-Lunden, P.J.H. Builtjes, S. Dutchak, J.H. Duyzer, S.E. Gryning, K.C. Jones, H.F.G. van Dijk, J.A. van Jaarsveld, Atmospheric transport and deposition of pesticides: an assessment of current knowledge, in: Workshop on Fate of Pesticides in the Atmosphere Implications for Risk Assessment, Kluwer Academic Publication, Driebergen, Netherlands, 1998, pp. 245–256.
[2] K.T. Whitby, Physical characteristics of sulfur aerosols, Atmos. Environ. 12 (1978) 135–159.
[3] W.T. Tsai, Y. Cohen, H. Sakugawa, I.R. Kaplan, Dynamic partitioning of semivolatile organics in gas particle rain phases during rain scavenging, Environ. Sci. Technol. 25 (1991) 2012–2023.
[4] M. Millet, H. Wortham, A. Sanusi, P. Mirabel, Atmospheric contamination by pesticides: determination in the liquid, gaseous and particulate phases, Environ. Sci. Pollut. Res. (1997) 172–180.
[5] F. van den Berg, R. Kubiak, W.G. Benjey, M.S. Majewski, S.R. Yates, G.L. Reeves, J.H. Smelt, A.M.A. van der Linden, Emission of pesticides into the air, in: Workshop on Fate of Pesticides in the Atmosphere Implications for Risk Assessment, Kluwer Academic Publication, Driebergen, Netherlands, 1998, pp. 195–218.
[6] R. Atkinson, R. Guicherit, R.A. Hites, W.U. Palm, J.N. Seiber, P. de Voogt, Transformations of pesticides in the atmosphere: a state of the art, in: Workshop on Fate of Pesticides in the Atmosphere Implications for Risk Assessment, Kluwer Academic Publication, Driebergen, Netherlands, 1998, pp. 219–243.
[7] T.F. Bidleman, Atmospheric processes – wet and dry deposition of organic-compounds are controlled by their vapor particle partitioning, Environ. Sci. Technol. 22 (1988) 361–367.
[8] T.P. Klupinski, Y.P. Chin, Abiotic degradation of trifluralin by Fe(II): kinetics and transformation pathways, Environ. Sci. Technol. 37 (2003) 1311–1318.
[9] C. Bedos, M.F. Rousseau-Djabri, B. Gabrielle, D. Flura, B. Durand, E. Barriuso, P. Cellier, Measurement of trifluralin volatilization in the field: Relation to soil residue and effect of soil incorporation, Environ. Pollut. 144 (2006) 958–966.
[10] R. Grover, J.D. Wolt, A.J. Cessna, H.B. Schiefer, Environmental fate of trifluralin, Rev. Environ. Contam. Toxicol. 153 (1997) 1–64.
[11] A. Scheyer, S. Morville, P. Mirabel, M. Millet, Variability of atmospheric pesticide concentrations between urban and rural areas during intensive pesticide application, Atmos. Environ. 41 (2007) 3604–3618.
[12] S.M. Chernyak, C.P. Rice, L.L. McConnell, Evidence of currently used pesticides in air, ice, fog, seawater and surface microlayer in the Bering and Chukchi seas, Mar. Pollut. Bull. 32 (1996) 410–419.
[13] H.F.G. van Dijk, R. Guicherit, Atmospheric dispersion of current-use pesticides: a review of the evidence from monitoring studies, in: Workshop on Fate of Pesticides in the Atmosphere Implications for Risk Assessment, Kluwer Academic Publication, Driebergen, Netherlands, 1998, pp. 21–70.
[14] S.B. Hawthorne, D.J. Miller, P.K.K. Louie, R.D. Butler, G.G. Mayer, Vapor-phase and particulate-associated pesticides and PCB concentrations in eastern North Dakota air samples, J. Environ. Qual. 25 (1996) 594–600.
[15] C.S. Helling, Dinitroaniline herbicides in soils, J. Environ. Qual. 5 (1976) 1–15.
[16] E. Leitis, D.G. Crosby, Photodecomposition of trifluralin, J. Agric. Food Chem. 22 (1974) 842–848.
[17] C.J. Soderquist, D.G. Crosby, K.W. Moilanen, J.N. Seiber, J.E. Woodrow, Occurrence of trifluralin and its photoproducts in air, J. Agric. Food Chem. 23 (1975) 304–309.
[18] T. Golab, W.A. Althaus, H.L. Wooten, Fate of trifluralin-C-14 in soil, J. Agric. Food Chem. 27 (1979) 163–179.
[19] G.W. Probst, T. Golab, R.J. Herberg, F.J. Holzer, S.J. Parka, C. Van der Schans, J.B. Tepe, Fate of trifluralin in soils and plants, J. Agric. Food Chem. 15 (1967) 592–599.
[20] A.C. Pierpoint, C.J. Hapeman, A. Torrents, Ozone treatment of soil contaminated with aniline and trifluralin, Chemosphere 50 (2003) 1025–1034.
[21] A. Le Person, A. Mellouki, A. Munoz, E. Borras, M. Martin-Reviejo, K. Wirtz, Trifluralin: photolysis under sunlight conditions and reaction with HO radicals, Chemosphere 67 (2007) 376–383.
[22] D. Bossan, H. Wortham, P. Masclet, Atmospheric transport of pesticides adsorbed on aerosols. 1. Photodegradation in simulated atmosphere, Chemosphere 30 (1995) 21–29.
[23] J.N. Shu, S.K. Gao, Y. Li, A VUV photoionization aerosol time-of-flight mass spectrometer with a RF-powered VUV lamp for laboratory-based organic aerosol measurements, Aerosol Sci. Technol. 42 (2008) 110–113.
[24] N.O.A. Kwamena, M.G. Staikova, D.J. Donaldson, I.J. George, J.P.D. Abbatt, Role of the aerosol substrate in the heterogeneous ozonation reactions of surface-bound PAHs, J. Phys. Chem. A 111 (2007) 11050–11058.
[25] D.H. Giamalva, D.F. Church, W.A. Pryor, Kinetics of ozonation. 6. Polycyclic aliphatic-hydrocarbons, J. Org. Chem. 53 (1988) 3429–3432.
[26] E. Proksch, A.D. Meijere, Oxidation of cyclopropyl hydrocarbons with ozone, Angew. Chem. Int. Ed. 15 (1976) 761–762.